



Multi-shape registration with constrained deformations

Rosa Kowalewski, Barbara Gris

► To cite this version:

Rosa Kowalewski, Barbara Gris. Multi-shape registration with constrained deformations. GSI 2021 - 5th International Conference Geometric Science of Information, Jul 2021, Paris, France. pp.82-90, 10.1007/978-3-030-80209-7_10 . hal-03251766v2

HAL Id: hal-03251766

<https://hal.science/hal-03251766v2>

Submitted on 12 Jan 2022

HAL is a multi-disciplinary open access archive for the deposit and dissemination of scientific research documents, whether they are published or not. The documents may come from teaching and research institutions in France or abroad, or from public or private research centers.

L'archive ouverte pluridisciplinaire **HAL**, est destinée au dépôt et à la diffusion de documents scientifiques de niveau recherche, publiés ou non, émanant des établissements d'enseignement et de recherche français ou étrangers, des laboratoires publics ou privés.

Multi-shape registration with constrained deformations

Rosa Kowalewski¹[0000–0003–1939–222X]* and Barbara Gris²[0000–0001–9440–3879]

¹ University of Bath, BA2 7AY, UK

² Laboratoire Jacques-Louis Lions, Sorbonne Université, 75005 Paris, France

Abstract. Based on a Sub-Riemannian framework, deformation modules provide a way of building large diffeomorphic deformations satisfying a given geometrical structure. This allows to incorporate prior knowledge about object deformations into the model as a means of regularisation [10]. However, diffeomorphic deformations can lead to deceiving results if the deformed object is composed of several shapes which are close to each other but require drastically different deformations. For the related Large Deformation Diffeomorphic Metric Mapping, which yields unstructured deformations, this issue was addressed in [2] introducing object boundary constraints. We develop a new registration problem, marrying the two frameworks to allow for different constrained deformations in different coupled shapes.

Keywords: Shape registration · Large deformations · Sub-Riemannian geometry.

1 Introduction

The improvement of medical imaging techniques increase the need for automatic tools to analyse the generated data. Matching two shapes (curves, images) in order to understand the differences or the evolution between two observations is often a key step. Large deformations, defined as flows of time-dependent vector fields [9, 5], allow to perform efficient shape registration [4, 6, 12]. In some cases, in order to analyse the estimated deformation, it is required to only consider a subset of suitable deformations [10, 14–16]. In addition, the regularity of such deformations often prevents the simultaneous registration of several shapes close to each other, but requiring different types of motions, as it appears in medical imaging (with several organs for instance, see [13]). We present in this article a *modular multi-shape registration framework*, combining the deformation module framework [10] with multi-shape registration [2].

* Rosa Kowalewski is supported by a scholarship from the EPSRC Centre for Doctoral Training in Statistical Applied Mathematics at Bath (SAMBa), under the project EP/S022945/1.

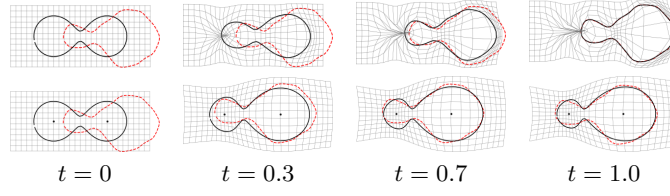


Fig. 1: Registration of unparametrized curves using LDDMM (top) and deformation modules (bottom). The red dotted curve is the target, the black curve the evolving shape. The two points are the centers of the local scaling.

2 Background

2.1 Structured large deformations

A strategy to restrict large deformations to an appropriate subset is to incorporate a structure in the deformation model via chosen field generators [10, 14, 16, 17] or constraints [1]. We will use here a simplified version of the deformation module framework [10] which allows to build an appropriate vocabulary of interpretable fields. A deformation module is defined as a quadruple $(\mathcal{O}, H, \zeta, c)$. The field generator $\zeta : \mathcal{O} \times H \mapsto C_0^l(\Omega, \mathbb{R}^d)$, allows to parameterise structured vector fields such as local scaling, or physically motivated deformations. The *geometrical descriptor* $q \in \mathcal{O}$ contains the 'geometrical information' of the generated vector field, such as its location. In this article we will assume \mathcal{O} is a space of landmarks of \mathbb{R}^d , which includes the case of discretised curves. The *control* $h \in H$ selects a particular field amongst the allowed ones. Finally, the *cost* function $c : \mathcal{O} \times H \mapsto \mathbb{R}^+$ associates a cost to each couple in $\mathcal{O} \times H$. Under some conditions (see section 3), the trajectory $\zeta_{q_t}(h_t)$ can be integrated via the flow equation $\dot{\varphi}_t = \zeta_{q_t}(h_t) \circ \varphi_t$, $\varphi_{t=0} = Id$, so that the structure imposed on vector fields can be transferred to a structure imposed on large deformations [10]. The evolution of q is then given by $\dot{q}_t = \zeta_{q_t}(h_t)(q_t)$, where $v(q) = (v(x_1), \dots, v(x_p))$ if q consists of the points $x_i \in \mathbb{R}^d$. The framework comes with the possibility to combine several deformation modules $\mathcal{M}^i = (\mathcal{O}^i, H^i, \zeta^i, c^i)$, $1 \leq i \leq N$, into the *compound module* $C(\mathcal{M}^1, \dots, \mathcal{M}^N) = (\mathcal{O}, H, \zeta, c)$ defined by $\mathcal{O} = \prod_i \mathcal{O}^i$, $H = \prod_i H^i$, $\zeta : (q, h) \mapsto \sum_i \zeta_{q^i}^i(h^i)$ and $c : (q, h) \mapsto \sum_i c_{q^i}^i(h^i)$ with $q = (q^1, \dots, q^N)$ and $h = (h^1, \dots, h^N)$. This combination enables to define a complex deformation structure as the superimposition of simple ones. Note that in modular large deformations generated by a compound module, each component q^i of the geometrical descriptor is transported by $\sum_i \zeta_{q^i}^i(h^i)$.

Figure 1 shows the result of the registrations of two unparametrized curves³ (modelled as varifolds [8]) with unstructured large deformations (with the Large Deformation Diffeomorphic Metric Mapping framework [5]) and modular ones. The deformation module is a compound module generating two scalings (one for

³ Data courtesy of Alain Trounev

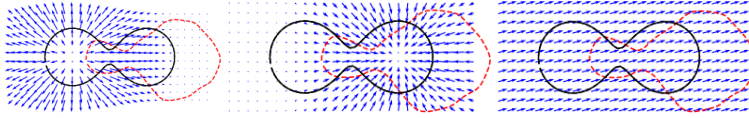


Fig. 2: Examples of vector fields generated by the scaling (left and middle) and translation (right) deformation modules.

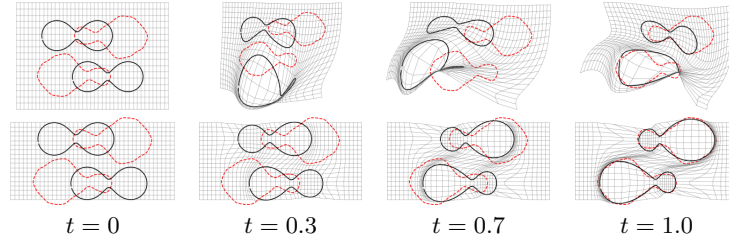


Fig. 3: Simultaneous registration using compound modules with single-shape (top) and multi-shape (bottom) frameworks. The evolving shape is in black, the target in red.

each lobe) and a large scale local translation (translating the whole curve)⁴. Figure 2 shows examples of vector fields generated by these modules. Even though they both give good curve registration, the prior in the structure ensures that the modular deformation is composed of uniform scalings. In addition, each component of the global deformation can be studied separately [7, 18].

2.2 Multi-Shape Registration

Deformation modules generate smooth deformations, modelling shapes as one homogeneous medium. Studying multiple shapes using one diffeomorphism leads to huge interactions between the shapes as they are moving close. Performing a simultaneous registration using a compound module leads to unsatisfying results due to the close location of shapes, as in figure 3.

To solve this problem, it would be desirable to have the deformation module for each shape only deform the inside of the curve, without influencing the deformation outside, while maintaining consistency between deformations. The multi-shape registration framework introduced in [2] addresses this problem for the LDDMM framework [5], by considering deformations for each subshape and linking them at the boundaries. In general, N source and corresponding target shapes q_S^i and q_T^i , $i = 1, \dots, N$ are considered. Each shape q^i is associated with an open set U^i of \mathbb{R}^d such that $q^i \subset U^i$, $\cup \bar{U}^i = \mathbb{R}^d$ and $U^i \cap U^j = \emptyset$ if $i \neq j$. For curves, for example, the shape q^i represents the boundary of U^i . The total deformation is defined by $\varphi : x \in \mathbb{R}^d \mapsto \varphi^i(x)$ if $x \in U^i$.

In order to ensure the consistency at boundaries ∂U^i , such as continuity or prevention of overlapping deformations, authors introduce a continuous con-

⁴ For a more detailed description of how these modules are built, we refer to [10].

straints operator $C: \mathcal{O} \rightarrow L(V, Y)$ where $V = \prod_i V_i$, V_i is a space of vector fields for each i , Y is a Banach space and $L(V, Y)$ is the set of continuous linear operators between V and Y . Furthermore, consider a continuous function $\mathcal{D}: (\prod_i \mathcal{O}^i)^2 \rightarrow \mathbb{R}_+$, measuring the similarity of shapes. The multi-shape registration problem [2] reads

$$\begin{aligned} \min_{v \in L^2([0,1], V)} \quad & \frac{1}{2} \sum_{i=1}^N \int_0^1 \|v_t^i\|_2^2 dt + \mathcal{D}(q_1^i, q_T^i) \\ \text{s.t.} \quad & \dot{q}_t^i = v_t^i(q_t^i), \quad q_0 = q_S, \quad \text{and} \quad C_{q_t} v_t = 0. \end{aligned}$$

Two different types of constraints C_q have been introduced in [2]: identity constraints (modelling shapes 'stitched' to each other at the boundaries), and sliding constraints (allowing slidings between shapes tangential to the boundary).

3 Modular Multi-Shape Registration Problem

In order to address the case where the shapes under study are composed of several subshapes whose deformations should satisfy a certain structures, we design here a modular multi-shape registration framework. Let us consider N shapes and N deformation modules. Following [2], each of these shapes will be displaced by a modular large deformation generated by the associated module. We impose boundary constraints to ensure consistent combination of the deformations. The modular multi-shape registration problem is stated as follows.

Problem 1. Let $\mathcal{M}^i = (\mathcal{O}^i, H^i, \zeta^i, c^i)$, $i = 1, \dots, N$, be N deformation modules and $C: \prod_i \mathcal{O}^i \mapsto L(V, Y)$ be a continuous constraints operator with $V = \prod_i V_i$, V_i RKHS of vector fields and Y a finite dimensional vector space. Let q_S and q_T in $\prod_i \mathcal{O}^i$ and let $\mathcal{D}: (\prod_i \mathcal{O}^i)^2 \rightarrow \mathbb{R}_+$ be continuous. Minimise the functional

$$\mathcal{J}(q, h) = \frac{1}{2} \sum_{i=1}^N \int_0^1 c_{q_t^i}^i(h_t^i) dt + \mathcal{D}(q_{t=1}, q_T) \quad (1)$$

with respect to $q = (q^1, \dots, q^N)$ and $h = (h^1, \dots, h^N)$, with, $q_{t=0} = q_S$, for almost every t in $[0, 1]$, $C_{q_t} \zeta_{q_t}(h_t) = 0$ and for all i , $\dot{q}_t^i = \zeta_{q_t^i}^i(h_t^i)(q_t^i)$.

To formalize it, we introduce the *external combination* of deformation modules.

Definition 1 (External Combination of Deformation Modules). Let $\mathcal{M}^i = (\mathcal{O}^i, H^i, \zeta^i, c^i)$, $i = 1, \dots, N$ be C^k -deformation modules on \mathbb{R}^d of order l . Then their external combination $M(\mathcal{M}^1, \dots, \mathcal{M}^N)$ is the quintuplet $(\mathcal{O}, H, F, X, c)$ where $\mathcal{O} = \prod_i \mathcal{O}^i$, $H = \prod_i H^i$, $F: (q, h) \in \mathcal{O} \times H \mapsto (\zeta^1(q^1, h^1), \dots, \zeta^N(q^N, h^N)) \in \prod_i C_0^{l^i}(\mathbb{R}^{d_i}, \mathbb{R}^{d_i})$, $X: (q, v) \in \prod_i C_0^{l^i}(\mathbb{R}^{d_i}, \mathbb{R}^{d_i}) \times \mathcal{O} \rightarrow (v^1(q^1), \dots, v^N(q^N)) \in \prod_i T\mathcal{O}^i$ and cost $c_q(h) = \sum_i c_{q^i}^i(h^i): \mathcal{O} \times H \rightarrow c_q(h) \in \mathbb{R}_+$ where $q = (q^1, \dots, q^N)$, $h = (h^1, \dots, h^N)$ and $v = (v^1, \dots, v^N)$.

Remark 1. Unlike the compound module presented in section 2, the external combination does not result in a deformation module.

In the following, we will assume that all the deformation modules $(\mathcal{O}, H, \zeta, c)$ satisfy the *Uniform Embedding Condition* for a RKHS V continuously embedded in $C_0^1(\mathbb{R}^d)$ (UEC [10]) i.e. that there exists $\beta > 0$ such that for all $(q, h) \in \mathcal{O} \times H$, $\zeta_q(h)$ is in V and $|\zeta_q(h)|_V^2 \leq \beta c_q(h)$. An easy way to ensure it is to choose $c_q(h) = (1/\beta)|\zeta_q(h)|_V^2 + f(q, h)$ (with $f : \mathcal{O} \times H \rightarrow \mathbb{R}^+$ smooth), which is the case in the numerical examples in Section 4. In order to minimize equation (1), we first need to specify the trajectories (q, h) that will be considered.

Definition 2 (Constrained controlled path of finite energy).

Let $M(\mathcal{M}^1, \dots, \mathcal{M}^N) = (\mathcal{O}, H, F, X, c)$ be an external combination of the modules \mathcal{M}^i and let $C : \prod_i \mathcal{O}^i \mapsto L(V, Y)$ be a continuous constraints operator with $V = \prod_i V_i$, V_i RKHS of vector fields and Y a finite dimensional vector space. We denote by Ω the set of measurable curves $t \mapsto (q_t, h_t) \in \mathcal{O} \times H$ where q is absolutely continuous such that for almost every $t \in [0, 1]$, $\dot{q}_t = F_{q_t}(h_t)(q_t)$, $C_{q_t}\zeta_{q_t}(h_t) = 0$ and $E(q, h) := \int_0^1 c_{q_t}(h_t)dt < \infty$.

Remark 2. If $t \mapsto (q_t, h_t)$ is a constrained controlled path of finite energy of $M(\mathcal{M}^1, \dots, \mathcal{M}^N)$, each component q^i is displaced by the action of $\zeta_{q^i}^i(h^i)$ only, instead of the sum of all vector fields like in the compound module (section 2).

If (q, h) is in Ω , for each (q^i, h^i) a modular large deformation φ^i of \mathbb{R}^d as the flow of $\zeta_{q^i}^i(h^i)$ can be built [10, 11]. Then (see [3] and section 2.2), we can combine all φ^i into one deformation φ . If the constraints operator C prevents overlapping between sets $\varphi^i(U^i)$ and $\varphi^j(U^j)$, such as the aforementioned identity or sliding constraints, then φ defines a bijective deformation which respects the topology and the desired deformation structure within each set U^i . We show now that equation (1) has a minimiser on Ω .

Proposition 1. Let V_1, \dots, V_N be a N RKHS continuously embedded in $C_0^2(\mathbb{R}^d)$, and let for $i = 1, \dots, N$, $\mathcal{M}^i = (\mathcal{O}^i, H^i, \zeta^i, \xi^i, c^i)$ be deformation modules satisfying the UEC for V_i . Let $\mathcal{D} : \mathcal{O} \times \mathcal{O} \mapsto \mathbb{R}^+$ be continuous. Let q_S and $q_T \in \mathcal{O} := \prod_i \mathcal{O}^i$ and $C : \mathcal{O} \times V \mapsto Y$ be a constraints operator with Y a finite dimensional vector space. Then the minimiser of the energy $J(q, h) = \int_0^1 c_{q_t}(h_t)dt + \mathcal{D}(q_{t=1}, q_T)$ on $\{(q, h) \in \Omega \mid q_{t=0} = q_S\}$ exists.

We sketch the proof here and refer to [11] for a detailed version.

Proof. Let $(q^j, h^j)_j = ((q^{(i,j)}, h^{(i,j)})_{1 \leq i \leq N})_j$ be a minimising sequence in Ω . Up to successive extractions, we can suppose that for each i , $E^i((q^{(i,j)}, h^{(i,j)})) = \int_0^1 c_{q^{(i,j)}}^i(h^{(i,j)})$ converges to $E^{i,\infty}$. It can be shown similarly to [10] that $h^{(i,j)} \rightharpoonup h^{(i,\infty)}$ in $L^2([0, 1], H^i)$ and $q^{(i,j)} \rightarrow q^{(i,\infty)}$ uniformly on $[0, 1]$ with $(q^{(i,\infty)}, h^{(i,\infty)})$ absolutely continuous such that for almost every t , $\dot{q}_t^i = \zeta_{q_t^i}^i(h_t^i)(\dot{q}_t^i)$ and $E^i(q^{(i,\infty)}, h^{(i,\infty)}) \leq E^{i,\infty}$. Then with $(q^\infty, h^\infty) = (q^{(i,\infty)}, h^{(i,\infty)})_{1 \leq j \leq N} \in \Omega$, $\inf\{J(q, h) \mid (q, h) \in \Omega\} = \lim J(q^j, h^j) = J(q^\infty, h^\infty)$. In addition, it is shown in [10] that $F_{q^j}(h^j)$ converges weakly to $F_{q^\infty}(h^\infty)$, so (see [3]), $C_{q_t^\infty} \circ F_{q_t^\infty}(h_t^\infty) = 0$ for almost every t in $[0, 1]$ which concludes the proof.

Let us define the Hamiltonian function $\mathcal{H}: \mathcal{O} \times T_q \mathcal{O}^* \times H \times Y \rightarrow \mathbb{R}$ by

$$\mathcal{H}(q, p, h, \lambda) := (p|F_q(h)(q))_{T_q^* \mathcal{O}, T_q \mathcal{O}} - \frac{1}{2}(Z_q h|h)_{H^*, H} - (\lambda|C_q F_q(h))_{Y^*, Y},$$

where $Z_q: H \rightarrow H^*$ is the invertible symmetric operator such that $c_q(h) = (Z_q h|h)_{H^*, H}$ ([10]). Similarly to [3], it can be shown that minimising trajectories (q, h) are such that there exist absolutely continuous $p: t \in [0, 1] \mapsto T_{q_t}^* \mathcal{O}$ and $\lambda: t \mapsto F$ such that

$$\begin{aligned} \dot{q} &= \frac{\partial}{\partial p} \mathcal{H}(q, p, h, \lambda) & \dot{p} &= -\frac{\partial}{\partial q} \mathcal{H}(q, p, h, \lambda) \\ \frac{\partial}{\partial h} \mathcal{H}(q, p, h, \lambda) &= 0 & \frac{\partial}{\partial \lambda} \mathcal{H}(q, p, h, \lambda) &= 0. \end{aligned}$$

The last two equations can be solved, so that for minimising trajectories $h = Z_q^{-1}(\rho_q^* p - (C_q F_q)^* \lambda)$ and $\lambda = (C_q F_q Z_q^{-1} (C_q F_q)^*)^{-1} C_q F_q Z_q^{-1} \rho_q^* p$ with $\rho_q: h \in H \mapsto F_q(h)(q)$ and assuming $C_q F_q Z_q^{-1} (C_q F_q)^*$ is invertible. The previous system of equations has then a unique solution associated to each initial condition (q_0, p_0) . In order to minimise equation (1), we optimise it with respect to the initial momentum p_0 .

Proposition 2 ([11, 3]). *Let $C_q \zeta_q: H \rightarrow Y$ be surjective. Then the operator $C_q F_q Z_q^{-1} (C_q F_q)^*$ is invertible.*

Remark 3. The surjectivity of $C_q F_q$ is in general not guaranteed but is easily obtained in practice (see section 4).

Remark 4. Compared to the frameworks of (single-shape) structured deformations [7, 10] and multi-shape (unstructured) large deformations [2], it is necessary to inverse the operator $C_q F_q Z_q^{-1} (C_q F_q)^*$ at each time to compute the final deformation. This increases drastically the time-complexity and the memory print.

4 Numerical Results

In the practical study of multi-shapes, we encounter two main cases where a multi-shape setting is needed. For example, to study the motion of lungs and abdominal organs during the breath cycle, it is natural to model the organs as separate shapes embedded in a background which represents the surrounding tissue. On the other hand, if two organs are in contact, they can be modelled as several subshapes sharing a boundary. Here the boundary constraints are expressed only on the discretisation points (the convergence of this approximation is studied in the case of unstructured deformations in [2]). All the results here were generated using the library IMODAL [7].

Shapes in a background. We consider again the simultaneous registration of two peanut-shaped curves. They define three open sets (two bounded ones delimited by the curves, and the background) so we need to define three deformation

modules. For each curve q^i , $i = 1, 2$, we choose deformation modules modelling scalings of the left and right half, and a translation of the whole shape. We define the background shape as $q^3 = (q^{31}, q^{32})$, where $q^{31} = q^1$ and $q^{32} = q^2$, and the third deformation module is chosen to generate a sum of local translations carried by q^3 . We impose identity constraints on corresponding boundary points of each q^i and q^{3i} , with the constraints operator $C_q(v) = (v^1(q^1) - v^3(q^{31}), v^2(q^2) - v^3(q^{32}))$ with $v = (v^1, v^2, v^3)$. The unstructured background deformation module ensures that the operator $C_q F_q$ is surjective. Figure 3 shows the result of the multi-shape registration. The two curves move closely, without influencing each other. Unlike the compound module, the deformations inside the curves resemble the deformation we obtain from the registration of a single shape, see figure 1.

Subshapes with shared boundary. We consider two tree-shaped curves, modelled as varifolds [8], where the trunk of the source is thinner than the target’s while the crown of the source is larger (see Figure 4). Such differences require a multi-shape registration where a sliding is allowed at the boundary between the trunk and the crown. We place ourselves in the typical use case, registration of a synthetic segmented template to a new unsegmented subject. For each subshape (trunk and crown) we define a compound deformation module as the combination of 4 modules generating respectively a uniform horizontal scaling, a uniform vertical scaling, a global translation and a sum of local translations centered at the curve and boundary points (with a high penalty so that the deformation prior is only changed slightly). The last one ensures the surjectivity of the operator $C_q F_q$. Figure 4 shows the registration using the modular multi-shape framework. The interest of the sliding constraints can be seen in the grid deformation. In addition, similar to [7, 18] the trajectory of the controls can then be analysed to understand the difference between the two shapes.

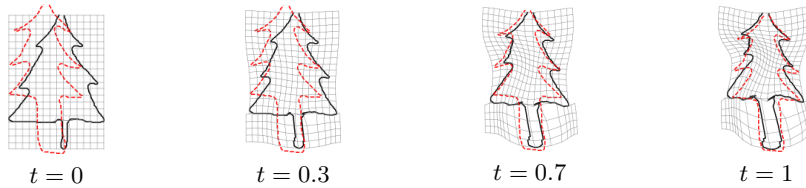


Fig. 4: registration of unparametrized curves with the modular multi-shape frameworks. The deformed (segmented) source is in black, the (unsegmented) target in red.

5 Conclusion

We have provided a framework and synthetic examples for using a vocabulary of structured deformations for multiple shape registration. In future work we will optimise our use of the IMODAL tools to improve the computation time

and memory print. There are promising perspectives for the application on, e.g., medical images with a known segmentation, in order to incorporate physical properties in different tissues and analyse the resulting registration.

References

1. Arguillere, S., Miller, M.I., Younes, L.: Diffeomorphic surface registration with atrophy constraints. *SIAM Journal on Imaging Sciences* **9**(3), 975–1003 (2016)
2. Arguillere, S., Trélat, E., Trouvé, A., Younes, L.: Multiple shape registration using constrained optimal control. *arXiv preprint arXiv:1503.00758* (2015)
3. Arguillere, S., Trélat, E., Trouvé, A., Younes, L.: Shape deformation analysis from the optimal control viewpoint. *Journal de mathématiques pures et appliquées* **104**(1), 139–178 (2015)
4. Ashburner, J.: Computational anatomy with the spm software. *Magnetic resonance imaging* **27**(8), 1163–1174 (2009)
5. Beg, M.F., Miller, M.I., Trouvé, A., Younes, L.: Computing large deformation metric mappings via geodesic flows of diffeomorphisms. *International journal of computer vision* **61**(2), 139–157 (2005)
6. Bône, A., Louis, M., Martin, B., Durrleman, S.: Deformetrica 4: an open-source software for statistical shape analysis. In: *International Workshop on Shape in Medical Imaging*. pp. 3–13. Springer (2018)
7. Charlier, B., Gris, B., Lacroix, L., Trouvé, A.: Imodal: creating learnable user-defined deformation models. In: *CVPR* (2021)
8. Charon, N., Trouvé, A.: The varifold representation of nonoriented shapes for diffeomorphic registration. *SIAM Journal on Imaging Sciences* **6**(4), 2547–2580 (2013)
9. Christensen, G.E., Rabbitt, R.D., Miller, M.I.: Deformable templates using large deformation kinematics. *IEEE transactions on image processing* **5**(10)
10. Gris, B., Durrleman, S., Trouvé, A.: A sub-riemannian modular framework for diffeomorphism-based analysis of shape ensembles. *SIAM Journal on Imaging Sciences* **11**(1), 802–833 (2018)
11. Kowalewski, R.: Modular Multi-Shape Registration. Master’s thesis, Universität zu Lübeck (2019)
12. Miller, M.I., Trouvé, A., Younes, L.: Hamiltonian systems and optimal control in computational anatomy: 100 years since d’arcy thompson. *Annual review of biomedical engineering* **17**, 447–509 (2015)
13. Risser, L., Vialard, F.X., Baluwala, H.Y., Schnabel, J.A.: Piecewise-diffeomorphic image registration: Application to the motion estimation between 3d ct lung images with sliding conditions. *Medical image analysis* **17**(2), 182–193 (2013)
14. Seiler, C., Pennec, X., Reyes, M.: Capturing the multiscale anatomical shape variability with polyaffine transformation trees. *Medical image analysis* **16**(7)
15. Sommer, S., Nielsen, M., Darkner, S., Pennec, X.: Higher-order momentum distributions and locally affine lddmm registration. *SIAM Journal on Imaging Sciences* **6**(1), 341–367 (2013)
16. Srivastava, A., Saini, S., Ding, Z., Grenander, U.: Maximum-likelihood estimation of biological growth variables. In: *International Workshop on Energy Minimization Methods in Computer Vision and Pattern Recognition*
17. Younes, L.: Constrained diffeomorphic shape evolution. *Foundations of Computational Mathematics* **12**(3), 295–325 (2012)
18. Younes, L., Gris, B., Trouvé, A.: Sub-riemannian methods in shape analysis. In: *Handbook of Variational Methods for Nonlinear Geometric Data*